Published in final edited form as:
*Exp Eye Res*. 2011 November ; 93(5): 700–709. doi:10.1016/j.exer.2011.09.001.

# Localization and phenotype-specific expression of ryanodine calcium release channels in C57BL6 and DBA/2J mouse strains

**Wei Huang**[1], **Wei Xing**[1], **Daniel A. Ryskamp**[1], **Claudio Punzo**[2], and **David Križaj**[1]

[1]Department of Ophthalmology & Visual Sciences, John A. Moran Eye Center, University of Utah School of Medicine, Salt Lake City, UT 84132

[2]Department of Ophthalmology, University of Massachusetts Medical School, Worcester, MA 01605

## Abstract

The DBA/2J (D2) and C57BL6 (B6) mouse strains are widely used in research as models for anxiety, addiction and chronic glaucoma. D2, but not B6, animals develop elevated intraocular pressure (IOP) that leads to progressive degeneration of retinal ganglion cell (RGC) axons and perikarya. Here we compare the expression and localization of intracellular ryanodine receptor (RyR) $Ca^{2+}$ store mechanisms in retinas from D2 and B6 animals. A subset of experiments included retinas from D2-*Gpnmb*$^{+}$ mice as strain-specific controls for D2s. RT-PCR analysis showed 6–8 -fold upregulation RyR1, but not RyR2 or RyR3 transcripts, in D2 retinas. The upregulation was more pronounced in D2 retinas categorized as exhibiting moderate or severe glaucoma eyes compared to eyes with no/little glaucoma. In B6 retinas, RyR1 was expressed in neuronal perikarya/processes across all three retinal layers whereas little labeling was observed in astrocyte, microglial or Müller cell processes. In contrast, RyR1 antibodies strongly labeled radial processes of in D2 Müller glia, in which the staining colocalized with the activated glial stress marker GFAP. RyR1 staining in 1 month-old D2-*Gpnmb*$^{+}$ strain resembled expression in B6 retinas whereas moderate RyR1, but not GFAP, localization to Müller glia was observed in 10–12 months - old D2-*Gpnmb*$^{+}$ eyes. Both RyR1-ir and GFAP-ir were augmented in the microbead injection model of acute experimental glaucoma. We conclude that RyR1 exhibits differential expression and localization in two ubiquitously used mouse lines. While RyR1 signals can be regulated in a strain-specific manner, our data also suggest that RyR1 transcription is induced by early glial activation and/or elevation in intraocular pressure.

### Keywords

calcium; ryanodine receptor; retina; Mueller glia; glaucoma; C57BL6; DBA/2J-Gpnmb$^{+}$ strain

## Introduction

It is increasingly evident that glaucoma is a multifactorial disease involving complex interactions between multiple genes, vascular factors, innate and adaptive immune system



Corresponding author: Dr. David Krizaj, Dept. of Ophthalmology & Visual Sciences, Moran Eye Center, Univ. of Utah School of Medicine, Salt Lake City, UT 84132, Tel: 801-213-2777, Fax: 801-587-8314, david.krizaj@hsc.utah.edu.

and environmental factors (Gordon et al., 2002). Many features of the human disease have been replicated in mouse models of chronic glaucoma. The most widely used DBA/2J (D2) mouse strain is characterized by recessive mutations in *Gpnmb* (*Gpnmb*$^{R150X}$) and *Tyrp1* (*Tyrp1*$^{b}$) genes which cause an increase in IOP at >6 months (John et al., 1998; Libby et al., 2005). D2 animals consequently express a phenotype that is similar to the chronic age-related glaucoma in humans with increased intraocular pressure (IOP), progressive degeneration of retinal axons, loss of RGC perikarya, glial activation, retinal remodeling and excavation of the optic nerve head (Anderson et al., 2002; Danias et al., 2003; Libby et al., 2005; Soto et al., 2008).

The D2 phenotype includes multiple contributions from genes that are distinct from the two mutations that regulate aqueous outflow in the anterior chamber. For example, the D2 strain varies from the B6 strain that is commonly used as a “wild type” strain in terms of anxiety, locomotor behavior, visual behavior, hippocampus-dependent learning performance, addiction, water consumption, life span and susceptibilities to a wide variety of stresses (Belzung and Griebel, 2001; Lucki et al., 2001; Puk et al., 2007; Barabas et al., 2011). At least 77 genes and ESTs show >1.5-fold mean increase in brains of adult B6 compared to D2 mice, with particular changes in genes that regulate signaling pathways, gene regulation and metabolism (Misra et al., 2007; Singh et al., 2007). With respect to calcium regulation, B6 and D2 tissue differ in expression of several $Ca^{2+}$-associated proteins that include ionotropic glutamate receptors (NMDA2B), voltage-operated $Ca^{2+}$ channels, calcium/calmodulin-dependent protein kinase II (CamKII), calcineurin phosphatases, inositol triphosphate receptors and a MAP kinase (Esplin et al., 1994; Grice et al., 2006). We focused on ryanodine receptors (RyRs) which play a crucial role in neuronal function as well as in the etiology of neurodegenerative diseases such as Alzheimer, Parkinson’s, Huntingdon’s diseases and spinocerebellar ataxia (Guo et al., 2010; Kasumu and Bezprozvannyi, 2010). $Ca^{2+}$ release from ryanodine stores amplifies $Ca^{2+}$-dependent signals induced by voltage-operated, glutamatergic and purinergic signals resulting in increased excitability of neuronal/glial cells (Nedergaard et al., 2010). Given that ryanodine signaling in optic astrocytes is directly activated by hydrostatic pressure (Mandal et al., 2010) and that D2 animals develop glaucoma following persistent elevation in IOP (John et al., 1998; Libby et al., 2005; Soto et al., 2008), it would seem important to determine whether RyR expression and cellular localization are affected in D2 mice. Because the expression and localization of ryanodine receptor isoforms in the mouse retina are not known, we first compared the abundance of RyR transcripts in B6 and D2 retinas and determined the localization of the two main retinal RyR isoforms in the mouse retina. We also tested the hypothesis that the dramatic phenotype observed in D2 animals derives, in part, from elevation in IOP.

Our data show that the two strains exhibit marked differences in the expression of genes coding for RyR1, but not RyR2 or RyR3, isoforms. The D2 phenotype was associated with a shift in RyR1 expression to activated Müller astroglia. Similar shifts were observed following experimental elevation of IOP, suggesting that RyR signaling might be associated with glial activation in mechanically stressed retinas.

## Methods

### Animals

Animals were maintained in a pathogen-free facility under a 12-hour light–dark cycle (Utah) and 14 hour light/10 hour dark cycle (Jackson) with standard rodent chow available *ad libitum*. D2 and D2-*Gpnmb*$^{+}$ mice were obtained from The Jackson Laboratory and/or from Dr. Simon John’s (JAX) colony. The D2-*Gpnmb*$^{+}$ mice are homozygous for a wild-type allele of *Gpnmb* on a D2 genetic background. The strain develops iris disease similar to that in D2s but does not develop increased IOP or axonal degeneration (Howell et al., 2007). In

contrast, aging D2 animals show progressive loss of RGC markers and loss of RGCs (John et al., 1998; Howell et al., 2007; Barabas et al., 2011). Mice were aged at both sites; mice older than 12 months were aged exclusively at University of Utah. There were no obvious differences between mice aged to 12 months at each site. All experiments adhered to the NIH Guide for the Care and Use of Laboratory Animals and the ARVO Statement for the Use of Animals in Ophthalmic and Vision Research and were approved by the Institutional Animal Care and Use Committee at the University of Utah.

### Semiquantitative RT-PCR

Total RNA from retina was extracted with Trizol and total RNA was converted to cDNA using the SuperScript III First-Strand Synthesis kit from Invitrogen. Real-time PCR was performed on a thermocycler (GeneAmp 5700; ABI, Foster City, CA) using Power SYBR Green PCR Master Mix (Applied Biosystems, Foster City, CA) reagents according to the manufacturer's instructions. Table I lists the primers used. Two sets of primers were used for identification of the RyR1 isoform. After amplification, the ratio of gene-of-interest mRNA to glyceraldehyde-3-phosphate dehydrogenase (*Gapdh*) reference gene was calculated for each sample. A random sample at in the 1-month cohort was assigned a value of 1 and other values calculated relative to the sample. Every experiment consisted of samples from at least 5 animals, each gene was studied in 3 – 5 separate experiments.

### In situ hybridization

In situ hybridization and probe synthesis were performed as described previously [27]. Sp6 RNA polymerase was used to generate the probes. The probes were generated by sub-cloning part of the coding sequence into pGEMT-Easy (Promega). The forward primer for *RyR1* was: AGAGGGCGATGAAGATGAGAA; reverse primer: AAGATGTCCCCGTGTTTGTC. The forward primer for *RyR2* was AAACACCAGCCTTCGGAGTA; the reverse primer was TAGCCAAAGATGGGAAGGTG (Table I). For cryosections, the eyes were dissected in PBS (0.1M Phosphate Buffer solution), fixed in 4% PFA (Paraformaldehyde)/PBS at RT, washed with PBS and equilibrated in 10 min steps of increasing concentrations of sucrose (5 – 30%). The tissue was embedded in 1:1 mixture of OCT and 30% sucrose in PBS for 15 min and freeze dryed in dry ice/ethanol. For paraffin sections, retinas were fixed for 30 min in 4% PF/PBS at RT, washed with PBS and dehydrated to 100% ethanol using a ladder of increased EtOH concentrations before embedding in 50/50 xylene/paraffin (60 deg; 15 min) and 100% paraffin (4 × 30 min at 60 deg C).

### Tonometer Measurements

IOP was measured in mice between 10:00 AM and 1:00 PM with the TonoLab rebound tonometer (Colonial Medical Supply, Franconia, NH/Tyolat, Helsinki, Finland). Mice were sedated with intraperitoneal injection of Avertin with final amount calculated by weight (e.g., 0.5 ml for 21–24g animals). Animals were placed on a jack stand platform and the tonolab was clamped on a ring stand and centered onto the mid-cornea. During measurements animal were neither restrained nor touched. Each eye was measured twenty consecutive times, the highest and lowest values were discarded and the values were averaged. At 1 month, the pooled mean IOP for D2 eyes was not significantly different from B6 eyes (12.80 ± 0.55 vs. 12.08 ± 0.64 mm Hg). At 9 months, IOP levels in D2 eyes were significantly increased with respect to B6 eyes (21.50 ± 1.58 vs. 11.0 ± 0.66 mm Hg, N= 15; $P<0.001$; Mann-Whitney unpaired test).

### Immunohistochemistry

Immunostaining followed previously described protocols (Renteria et al., 2005; Ryskamp et al., 2011). Fixed transverse sections of the retina were washed in PBS for 15 min before permeabilization and blocking with 0.5% Triton X-100 and 10% goat serum. The slides were incubated with primary antibodies in the blocking solution for 4 hours at RT, washed twice in PBS and subsequently incubated for 4 hours with secondary antibodies. The primary antibodies utilized in the study were anti-RyR1 (rabbit polyclonal; 1:100, Millipore/Chemicon AB9078, Temecula, CA) raised against a peptide from human RyR1; as per manufacturers datasheet, in Western blots the antibody produces a band at the appropriate M.W. (also, see Medina-Ortiz et al., 2007). The anti-RyR2 (rabbit polyclonal; Millipore/Chemicon AB9080) antibody was derived from a synthetic peptide based on human protein and has been characterized previously (Garcia-Perez et al., 2008). The anti-GFAP (mouse monoclonal; 1:500; Sigma); anti-glutamine synthetase (mouse monoclonal; 1:1000; BD Biosciences) and anti-Brn3a (mouse monoclonal; 1:100; Santa Cruz Biotechnology) have been well characterized. The secondary antibodies were goat anti-mouse or goat anti-rabbit IgG (H+L) conjugated to fluorophores (Alexa 488 and Alexa 594 (Invitrogen), diluted 1:500 or 1:1000, goat anti-mouse Cy3 from Jackson ImmunoResearch at 1:1000 or Mac1-CD11b-AlexaFluor 488 from BD Pharmingen at 1:200. After incubation, sections on slides were washed in PBS and mounted using Vectashield (Vector, Burlingame, CA). Negative controls without a primary antibody showed no staining. Immunofluorescent and differential interference contrast (DIC) images were acquired at depths of 12 bits on a confocal microscope (Zeiss LSM 510) using 488 nm Ar (10%) and 594 nm He/Ne (100%) lines for fluorophore excitation, suitable band-pass or long-pass filters for emission detection and 40×/1.2 NA oil objectives. The analysis was performed in sections obtained from at least 3 animals at each age examined.

### Microbead injection

The injection protocol roughly followed the procedure described in Chen et al. (2011). During the proceeding week prior to experimentally elevating IOP, IOP was measured two or three times to establish a baseline. In preparation for the microbead injection procedure, pupils were dilated with 1% tropicamide (Bausch & Lomb, Rochester, NY) and mice were deeply sedated with an intraperitoneal injection of Ketamine/Xylazine (90 mg/10 mg per kg body weight). Heat pads were used to maintain body temperature. 0.5% proparacaine (Bausch & Lomb) was applied to the eyes for topical analgesia. The cornea was punctured with a sharp needle and some of the aqueous humor was gently drained. Using a 5.0 μl syringe (Hamilton; Reno, NV), 2 μl of a microbead solution (polystyrene FluoSpheres with diameter of 15 μm at a concentration of $1 \times 10^7$ beads/ml in PBS; Invitrogen) was slowly injected into the anterior chamber of a randomly selected eye. 2 μl of PBS was injected into the other eye of each mouse as an internal control. Injected eyes were treated with 0.5% erythromycin (Bausch & Lomb) and mice were closely monitored until consciousness was regained. Mice were allowed to recover for 72 hours before biweekly IOP measurements resumed. Of 10 eyes injected with microbeads, 3 showed a persistent elevation in IOP compared to PBS-injected contralateral controls. These three were used for data shown in Figure 7.

### Axon damage assessment

The severity of glaucoma was assessed in PPD-labeled nerves using an established grading scheme (Howell et al., 2007). Eyes were classified with no or early (no detectable axon damage/loss compared to B6), moderate (10–50% damage) or severe (>50% damage) glaucoma. The total number of examined retinas was No/Early glaucoma (9 months, N=8; 12–15 months, N=3); Moderate (9 months, N=3; 12–15 months, N=3), Severe glaucoma (9 months, N=2; 12 months, N=4; 15 months, N=4).

## Results

In this study, we employed two strategies to gain deeper insight into the expression and distribution of intracellular transport mechanisms in the D2 retina. Semi-quantitative reverse transcription (RT)-PCR was used to compare total retinal mRNA content of transcripts coding for ryanodine receptor $Ca^{2+}$ release channels in B6 and D2 mice. In the second approach, *in situ* hybridization and immunohistochemistry were used to identify the retinal localization of RyR1, the intracellular $Ca^{2+}$ release channel that exhibited the most prominent upregulation of transcription in D2 retinas.

### RyR1 signals in the B6 retina

Real-time PCR on cDNAs isolated from intact tissue showed that mRNA for RyR isoform 1 is transcribed in the B6 strain (Fig. 1A). The *RyR1* antisense probe showed prominent signals within the inner nuclear (INL) and ganglion cell layers (RGCL) (Fig. 1B).

Broadly consistent with *in situ* hybridization results, RyR1 protein was localized across all retinal strata, along neuronal cell bodies in INL and RGCL and in dendrites and axons within the IPL and NFL (Fig. 1C). While RyR1 signals were never observed in outer segments (OSs) of rods or cones, RyR1 immunoreactivity (ir) was more pronounced in the ellipsoid/inner segment region (Fig. 1C, arrowheads) and was also observed in the ONL. RyR1-ir was stronger in the IPL sublamina a compared to sublamina b, suggesting that RyR1-mediated $Ca^{2+}$ release could be disproportionately associated with OFF retinal signaling. RyR1 staining colocalized with the RGC marker Brn3a (Fig. 1D). Consistent with previous observations in spinal motoneurons (Ouarduz et al., 2003), RyR1 signals were observed in the nerve fibre layer proximal to RGC somata and in unmyelinated axonal projections entering the ONH (Fig. 1C & D). Staining of the astrocyte-rich lamina that represents the transition zone from the ONH to the optic nerve was lower compared to the NFL, the proximal ONH and the myelinated portion of the nerve vitread from the retina (Fig. 1C & 2A). Axonal staining in B6 retinas was distinct from glutamine synthetase (GS)- and Glial Fibrillary Acidic Protein (GFAP) signals localized to Müller cell and astrocyte processes at the ILM (Figs. 1E–G). Given the recent demonstration of the protective role of complement inhibition in glaucomatous degeneration (Hibbs et al., 2011) we also tested whether RyR1s are localized to retinal microglial cells. However, no colocalization was observed between RyR1 and Mac-1:AlexaFluor-488 immunolabeled cells residing in the IPL (Fig. 1H).

B6 sections almost never evinced GFAP-ir in the IPL/INL or the ONH whereas the RyR1 antibody strongly labeled the NFL entering the optic cup (arrowheads in 2A) and fibers within the optic nerve. Accordingly, little colocalization with glutamine synthetase or GFAP was observed in the ONH (Fig. 2B). RyR1 labeling of the astrocyte-rich prelaminar region was always weak.

### RyR1 signals in D2 and D2-*Gpnmb*$^{+}$ retinas

D2 retinas expressed RyR1 mRNA (Fig. 3A) which was localized mainly to the INL (Fig. 3B). Retinas with severe glaucoma exhibited a trend towards higher RyR1 mRNA content compared to retinas with no or early glaucoma, almost reaching significance with respect to Severe vs. No/Early glaucoma (Fig. 3C).

In contrast to the highly uniform and reproducible immunostaining pattern in B6 retinas, RyR1 signals in D2 retinas were variable in terms of neuronal vs. glial expression. The anti-RyR1 antibody labeled thin radial processes in the inner retina of 9 month-old D2animals with no detectable axonal loss (“no or early glaucoma” ) (arrowheads; Fig. 3Di). Such RyR1-ir processes, which were rarely labeled in B6 retinas, extended from the ILM towards

the OPL. These signals colocalized with glutamine synthetase (Fig. 3H) and GFAP (Fig. 3D & F), an intermediate filament which represents an early glial marker for retinal stress and is upregulated in Müller cells following acute or chronic elevation in IOP (Lam et al., 2003; Xue et al., 2006). The intensity of RyR1-ir and GFAP-ir in radial processes appeared to be accentuated in retinas classified into 'moderate' (N=6) and 'severe' (N=12) axonal degeneration categories (Fig. 3E–I). In extreme cases of severe glaucoma, retinas exhibited characteristics typical of Phase 3 'remodeling' (Marc et al., 2003) with disappearance of RGC/displaced amacrine perikarya, depletion of the INL and hypertrophy of glial processes which encased the remaining neuronal perikarya and reinforced both retinal laminas (OLM & ILM; Fig. 3I). In such remodeled retinas, glial processes appeared to lose the RyR1 signal (Fig. Ii & ii), however, the sample size was limited (N=2 animals at 15 months of age with severe glial hypertrophy). Intensity of RyR1-ir in radial processes varied between individual retinas within each category; panels E and F display retinal sections from two eyes with moderate glaucoma that exhibited different amounts of RyR1 signal.

RyR1 staining in D2 eyes was emphasized in the ONH tissue surrounding the 'excavated' area in moderate and severe glaucomatous eyes (asterisk in Fig. 3K). We also investigated whether RyR1 signals in glaucomatous eyes are upregulated in astrocytes in addition to Müller glia. As shown in the inset of Fig. 3K, little colocalization was observed between the astrocyte marker and RyR1-immunopositive nerve processes within the optic lamina.

The appropriate control strain for D2 animals are D2-*Gpnmb*$^{+}$ mice which are homozygous for a wild-type allele of *Gpnmb* on the D2 genetic background. Similar to D2s, D2-*Gpnmb*$^{+}$ mice develop iris disease but do not exhibit increased IOP or axonal degeneration (Howell et al., 2007). Localization of RyR1 mRNA in D2-*Gpnmb*$^{+}$ retinas was similar to signals observed in B6 and D2 retinas (Fig. 4B). Likewise, the pattern of RyR1-ir and GFAP-ir in 1 month-old (N=3) and a subset of 10–12 month-old D2 -*Gpnmb*$^{+}$ retinas resembled the staining observed in B6 retinas (N=4/10) (Fig. 4C & D). However, the majority of 10–12 month-old D2 -*Gpnmb*$^{+}$retinal samples (6/10 animals ) exhibited RyR1-ir within processes that traversed the INL. These processes were GFAP-immunonegative (data not shown) but colocalized with the Müller glial marker glutamine synthetase (Fig. 4E–F). The intensity of RyR1-ir in such D2-*Gpnmb*$^{+}$ retinas was similar to signals seen in No/Early glaucoma D2 retinas (Fig. 3D). In contrast to D2 tissue, however, GFAP expression mirrored B6 signals in the majority of 10–12 month-old D2-*Gpnmb*$^{+}$eyes (N=8/10; Fig. 4D) whereas GFAP-ir processes extending into the INL were observed within circumscribed patches of two D2-*Gpnmb*$^{+}$retinas (data not shown). With respect to RyR1 staining, differences between RyR1 staining in 10–12 months-old D2-*Gpnmb*$^{+}$animals could reflect different animal subpopulations and/or differential responses to the loss of *Tyrp1*$^{b}$. Consistent with the latter hypothesis that suggests aging-dependent stress associated with iris disease, RyR1-ir was more pronounced in Müller cells from adult D2-*Gpnmb*$^{+}$samples compared to 1 month-old eyes.

## RyR1 mRNA is upregulated in D2 retinas

The RyR family is comprised of 3 isoforms (RyR1-3) that are ubiquitously expressed across neurons and glia. Real-time PCR on cDNAs isolated from intact B6 and D2 tissue showed that mRNAs for all 3 RyR isoforms are transcribed in both strains. *RyR1* mRNA levels in D2 retinas were consistently higher compared to B6 control retinas (Fig. 1). The upregulation was observed at 1 month after birth (6.94 ± 1.07 –fold increase over WT; $P<0.01$; Mann-Whitney unpaired test) and persisted up to 15 months, the most advanced age studied (5.33 ± 1.01-fold increase; $P<0.01$, Mann-Whitney unpaired test) (Fig. 1A). To determine whether *RyR1* upregulation was a strain-specific, was associated with elevated IOP or loss of the *Tyrp1*$^{b}$ gene, we analyzed two time points in retinas from D2-*Gpnmb*$^{+}$ mice. RyR1 expression in D2-*Gpnmb*$^{+}$retinas (N=4) was not significantly different from B6

retinas at 1 month, but showed an increase at 5 months that was significant compared to B6 (N=8) and D2 (N=6) eyes (P=0.0003; one-way ANOVA). Thus, at least in 1 month-old animals, transcription of *RyR1* is not affected by general strain-specific features and the differences must lie downstream of the mutant *Gpnmb* gene whereas RyR1 mRNA levels may be elevated in older animals, possibly reflecting a strain-dependent or *Tyrp1*$^{b}$-dependent phenotype.

### RyR1 is localized to glia in an acute glaucoma model

We next tested whether upregulation of RyR1 signals within glial cells was a IOP-dependent process. IOP in B6 eyes was elevated by injection of Alexa488 nm-conjugated microbeads (Chen et al., 2011). Fourteen days following injection, the IOP was elevated in injected eyes from 3/10 animals. In these eyes, the IOP was 23.57 ± 2.96 mm Hg compared to 12.93 ± 1.40 mm Hg in PBS-injected contralateral eyes (N=3; P=0.0047). GFAP immunoreactivity in Müller cells was enhanced in all microbead-injected eyes that exhibited elevated IOP (Fig. 6B), consistent with increased resistance to mechanical stress (Bringmann et al., 2009). In contrast to GFAP signals in D2 retinas which often showed patches of strong GFAP-ir interspersed with weaker staining, GFAP-ir in eyes exposed to experimentally-induced IOP elevations appeared to be uniform across the retina. Colocalization between GFAP and RyR1 signals was observed in the proximal retina (Fig. 6B), suggesting that glial activation in this glaucoma model is also associated with increased expression of RyR1. Taken together, this data shows that development of glaucoma is associated with isoform-specific changes in expression of intracellular $Ca^{2+}$ release channels.

### Expression and localization of the RyR2 isoform is unchanged in the D2 retina

The antisense riboprobe localized RyR2 transcripts to INL, RGCL and ONL regions (Fig. 7B). Similar to previously reported staining in the rabbit (Shoshan-Barmatz et al., 2007), RyR2 signals in the mouse were observed across all retinal layers with a predominant labeling of Brn3a-immunopositive perikarya in the RGCL and the nerve fiber layer (Fig. 7C & H). Localization of RyR2 in D2 retinas was similar to the localization observed in B6 eyes (Fig. 7E–I). RyR2 staining in D2 retinas did not overlap with glutamine synthetase-ir processes in the ONL (Fig. 7F) or GFAP-ir in the IPL (Fig. 7E), indicating low levels of RyR2 expression in activated Müller glia. At high confocal gains, weakly labeled RyR2 -ir signals that were difficult to distinguish from background labeling were occasionally observed in the IPL (Fig. 7I). This data suggests that RyR2 in the mouse retina is a predominantly neuronal isoform.

In contrast to *RyR1*, expression of the *RyR2* and RyR3 genes was relatively unchanged between 1 month and 15 month-old retinas of B6 and D2 eyes (Fig. 5B & C) excepting a transient increase that was measured for RyR2 at 5 months (1.72 ± 0.15 -fold; N=3; P < 0.001; Kruskal-Wallis nonparametric ANOVA). We also compared expression of RyR2 and RyR2 genes in 5 month-old D2-*Gpnmb*$^{+}$ retinas (N=4 for each strain) and observed no significant differences in expression for RyR2 (P=0.3418, one-way ANOVA) or RyR3 (P=0.7816; one-way ANOVA).

## Discussion

In this paper we determined the localization of RyR1 and RyR2 channels in the mouse retina and compared their expression between widely used “wild type” B6 and “glaucoma model” D2 mouse strains. We show that expression and localization of RyR1, but not RyR2, isoforms exhibit both strain-specific and IOP-dependent features, suggesting that RyRs contribute to pathological remodeling of neuronal-glial interfaces in chronic glaucoma.

RyR1 riboprobes and anti-RyR1 antibodies labeled neuronal perikarya together with cellular processes. This pattern of RyR1 immunoreactivity in the B6 mouse was largely consistent with previously reported data from the rabbit retina (Shoshan-Barmatz et al., 2007). In contrast to the rabbit in which the RyR1 antibody labeled the outer segment, RyR1 and RyR2 signals in mouse photoreceptors were mainly confined to the ER-rich inner segment and cell body regions. Thus, these channels are likely to participate in the well-known feedback between voltage-operated channels, ER and mitochondria (Krizaj et al., 2003). Another interesting feature of RyR1 immunoreactivity in the B6 mouse retina was the consistently stronger staining of the IPL sublamina b compared to the sublamina a, possibly suggesting a more prominent role for $Ca^{2+}$-induced $Ca^{2+}$ release (CICR) in the retinal OFF pathway.

Retinal RyR1 mRNA content was increased ~2.5-fold in 1 month-old D2 compared to B6 retinas, preceding the onset of iridocorneal angle closure, IOP elevation and degeneration of RGC axons (John et al., 1998; Danias et al., 2003; Libby et al., 2005; Inman et al., 2006). This effect was not observed in previous microarray studies of retinal gene expression, most likely because RT-PCR is more sensitive for detecting changes in gene expression (Steele et al., 2006; Guo et al., 2010); however, at least one study identified several genes associated with voltage-operated Ca2+ entry and ER signaling which could participate in CICR (Panagis et al. 2010). RyR1 upregulation in D2 retinas coincided with increased levels of GFAP and early glial activation, which precede the onset of increased IOP by several months (Inman and Horner, 2007). Several pieces of evidence suggest that RyR1 expression could play a role in the pathogenesis of glaucoma: (1) There was a consistent trend towards higher RyR1 mRNA transcript content in retinas categorized as expressing moderate/severe glaucoma compared to no/early glaucoma; (2) The abundance of RyR1 mRNA in D2 retinas was higher than in D2-Gpnmb$^{+}$ retinas; (3) The intensity of RyR1 signals in Müller glia coincided with the severity of glaucoma; and (4) The phenotype of retinas with experimentally-induced IOP elevations retinas was similar to the moderate/severe glaucoma phenotype in D2 retinas.

Given that the onset of RyR1 upregulation in D2 eyes coincided with appearance of GFAP signals in Müller glia, the regulation of the RyR1 gene is likely to be associated with activation of Muller glia rather than RGC death. Müller cells are in a good topographic position to be the first retinal cell type to sense and respond to changes in IOP through ER-rich endfeet which transduce mechanical stimulation through regenerative $[Ca^{2+}]i$ increases (Keirstead and Miller, 1995; Newman, 2001; Li et al., 2001). It is unclear whether Müller glial RyR channels are directly activated by hydrostatic pressure as reported for optic nerve astrocytes (e.g., Mandal et al., 2010) or by $Ca^{2+}$ influx through stretch- and pressure-sensitive plasma membrane channels (Puro, 1991; Lindkvist et al., 2010; Ryskamp et al., 2011). In either case, the astroglial response to mechanical and neurochemical stress is likely to include augmented CICR. Intracellular $Ca^{2+}$ release channels tend to malfunction at early stages of neurodegeneration (Nedergaard et al., 2010) and it is therefore not inconceivable that suppression of RyR-mediated amplification of intracellular $Ca^{2+}$ signals will be protective with respect to glial activation and gliotic remodeling observed in retinal ischemia, diabetic retinopathy and/or glaucoma (Marc et al., 2003; see also Frandsen and Schousboe, 1991; Niebauer and Gruenthal, 1999; Popescu et al., 2002; Stirling and Stys, 2010; Kawasu and Bezprozvannyi, 2010).

The increase in the expression of Müller cell RyRs fits the general context of upregulated $Ca^{2+}$-dependent signal transduction pathways in D2 retinas (reviewed in Whitmore et al., 2005; Crish and Calkins, 2010), early Müller cell activation in D2 retinas (Inman and Horner, 2007), augmented neuronal excitability and susceptibility to stress in D2 animals (Esplin et al., 1994) and the increasingly recognized role of glial RyRs in axonal injury

(Stirling and Stys, 2010). B6 and D2 mouse strains exhibit numerous differences in biochemistry, physiology and behavior, including higher levels of angiotensin AT1 receptors, GABA receptor/channels, endothelin and complement signaling in D2 animals (DuBois et al., 2006; Golding et al., 2011; Hibbs et al., 2011), lower levels of protein kinase C and COMT (Bowers et al., 1995; Grice et al., 2007) and differential expression of NMDA receptors, voltage-operated $Ca^{2+}$ channels and calcineurin (Esplin et al., 1994; Grice et al., 2007).

However, our data argue against a simple glaucoma vs. non-glaucoma dichotomy of retinal RyR1 and GFAP expression. The early upregulation of RyR1, *Gfap* and microglial markers in D2 retinas (Inman and Horner, 2007) suggests that at least part of the RyR1 expression phenotype might be derived from *Gpnmb* loss of function rather than glaucoma per se. This conjecture is supported by the observation that RyR1 mRNA levels were elevated in D2 animals that had not (yet) exhibited glaucomatous RGC degeneration. Furthermore, the expression pattern of RyR1 signals in a subset of adult D2-*Gpnmb*$^+$ mice suggests that their retinas differ from both B6 and D2 animals. In particular, RyR1 signals that were observed in some GFAP-immunonegative D2-*Gpnmb*$^+$ Müller cells indicate that the RyR1 gene may be expressed in the absence of glial activation. Consistent with our observations, Porciatti et al. (2010) have recently shown that B6 and D2-*Gpnmb*$^+$ eyes differentially respond to spatial contrast, manifesting differential strain-specific organization of inner retinal circuits. As expected, contrast gain control mechanisms also differed between B6 vs. D2, and D2 vs. D2-*Gpnmb*$^+$ eyes (Porciatti et al., 2010). It remains to be determined whether moderate RyR1 expression in Müller cells is associated with the D2 phenotype or whether the RyR1 gene is regulated by the mild IOP increase and iris disease observed in D2-*Gpnmb*$^+$ animals (Howell et al., 2007).

In contrast to consistent upregulation of RyR1, expression or localization of RyR2, the main neuronal and retinal isoform, did not change in D2 retinas. Likewise, RyR3, typically considered an embryonic/neonatal isoform expressed at low levels in non-neuronal tissues or co-expressed with RyR2 (Bertocchini et al., 1997), showed no changes in mRNA transcript levels in D2 animals (Fig. 7). We conclude that retinal intracellular $Ca^{2+}$ release channels express plasticity in terms of isoform-specificity, transcription and localization. RyR1 expression and localization is highly sensitive to genetic and environmental influences that include the strain, iris disease, retinal gliosis and acute or chronic changes in IOP.

## Acknowledgments

The work was supported by the National Institutes of Health (RO1EY13870, T32DC008553, P30EY014800), The Foundation Fighting Blindness, Knights Templar Eye Foundation, Moran TIGER award and by the unrestricted grant from Research to Prevent Blindness to the Moran Eye Center at the University of Utah. We thank Drs. Gareth Howell and Simon John (Jackson Labs and HHMI) for generously providing D2 and D2-*Gpnmb*$^+$ samples, for help in classification of D2 eyes and for illuminating discussions. We also thank Dr. Jessica Li (University of Utah) for teaching us to perform retinal microinjections.

## References

Anderson MG, Smith RS, Hawes NL, Zabaleta A, Chang B, Wiggs JL, John SW. Mutations in genes encoding melanosomal proteins cause pigmentary glaucoma in D2 mice. Nat Genet. 2002; 30(1): 81–85. [PubMed: 11743578]

Barabas P, Huang W, Howell G, Tian N, Rentería R, John SMW, Krizaj D. The optomotor head turning reflex in the D2 mouse. Invest Ophthalmol Vis Sci. 2011 July 14. in the press.

Belzung C, Griebel G. Measuring normal and pathological anxiety-like behaviour in mice: a review. Behav Brain Res. 2001; 125(1–2):141–149. [PubMed: 11682105]

Bertocchini F, Ovitt CE, Conti A, Barone V, Schöler HR, Bottinelli R, Reggiani C, Sorrentino V. Requirement for the ryanodine receptor type 3 for efficient contraction in neonatal skeletal muscles. EMBO J. 1997; 16:6956–6963. [PubMed: 9384575]

Bowers BJ, Christensen SC, Pauley JR, Paylor R, Yuva L, Dunbar SE, Wehner JM. Protein and molecular characterization of hippocampal protein kinase C in C57BL/6 and DBA/2 mice. J Neurochem. 1995; 64:2737–2746. [PubMed: 7760054]

Chen H, Wei X, Cho KS, Chen G, Sappington R, Calkins DJ, Chen DF. Optic neuropathy due to microbead-induced elevated intraocular pressure in the mouse. Invest Ophthalmol Vis Sci. 2011; 52:36–44. [PubMed: 20702815]

Crish SD, Calkins DJ. Neurodegeneration in glaucoma: progression and calcium-dependent intracellular mechanisms. Neuroscience. 2011; 176:1–11. [PubMed: 21187126]

Danias J, Lee KC, Zamora MF, Chen B, Shen F, Filippopoulos T, Su Y, Goldblum D, Podos SM, Mittag T. Quantitative analysis of retinal ganglion cell (RGC) loss in aging DBA/2NNia glaucomatous mice: comparison with RGC loss in aging C57/BL6 mice. Invest Ophthalmol Vis Sci. 2003; 44:5151–5162. [PubMed: 14638711]

DuBois DW, Perlegas A, Floyd DW, Weiner JL, McCool BA. Distinct functional characteristics of the lateral/basolateral amygdala GABAergic system in C57BL/6J and DBA/2J mice. J Pharmacol Exp Ther. 2006; 318:629–640. [PubMed: 16651400]

Esplin MS, Abbott JR, Smart ML, Burroughs AF, Frandsen TC, Litzinger MJ. Voltage-sensitive calcium channel development in epileptic DBA/2J mice suggests altered presynaptic function. Epilepsia. 1994; 35:911–914. [PubMed: 7925160]

Frandsen A, Schousboe A. Dantrolene prevents glutamate cytotoxicity and $Ca^{2+}$ release from intracellular stores in cultured cerebral cortical neurons. J Neurochem. 1991; 56:1075–1078. [PubMed: 1671584]

Golding BJ, Overall AD, Gard PR. Strain differences and the role of AT(1) receptor expression in anxiety. Int J Mol Epidemiol Genet. 2011; 2:51–55. [PubMed: 21537401]

Gordon MO, Beiser JA, Brandt JD, Heuer DK, Higginbotham EJ, Johnson CA, Keltner JL, Miller JP, Parrish RK, Wilson MR, Kass MA. The Ocular Hypertension Treatment Study: baseline factors that predict the onset of primary open-angle glaucoma. Arch Ophthalmol. 2002; 20:714–720. [PubMed: 12049575]

Grice DE, Reenilä I, Männistö PT, Brooks AI, Smith GG, Golden GT, Buxbaum JD, Berrettini WH. Transcriptional profiling of C57 and DBA strains of mice in the absence and presence of morphine. BMC Genomics. 2007; 8:76. [PubMed: 17367521]

Guo Q, Fu W, Sopher BL, Miller MW, Ware CB, Martin GM, Mattson MP. Increased vulnerability of hippocampal neurons to excitotoxic necrosis in presenilin-1 mutant knock-in mice. Nat Med. 1999; 5:101–106. [PubMed: 9883847]

Guo Y, Johnson EC, Cepurna WO, Dyck JA, Doser T, Morrison JC. Early gene expression changes in the retinal ganglion cell layer of a rat glaucoma model. Invest Ophthalmol Vis Sci. 2011; 52:1460–1473. [PubMed: 21051717]

Hibbs M, Stevens B, Barres BA, Clark AF, Libby RT, John SWM. Molecular clustering identifies complement and endothelin induction as early events in a mouse model of glaucoma. J Clin Invest. 2011; 121:1429–1444. [PubMed: 21383504]

Howell GR, Libby RT, Marchant JK, Wilson LA, Cosma IM, Smith RS, Anderson MG, John SW. Absence of glaucoma in D2 mice homozygous for wild-type versions of Gpnmb and Tyrp1. BMC Genet. 2007; 8:45. [PubMed: 17608931]

Huang W, Fileta J, Rawe I, Qu J, Grosskreutz CL. Calpain activation in experimental glaucoma. Invest Ophthalmol Vis Sci. 2010; 51:3049–3054. [PubMed: 20107181]

Inman DM, Horner PJ. Reactive nonproliferative gliosis predominates in a chronic mouse model of glaucoma. Glia. 2007; 55:942–953. [PubMed: 17457855]

John SW, Smith RS, Savinova OV, Hawes NL, Chang B, Turnbull D, Davisson M, Roderick TH, Heckenlively JR. Essential iris atrophy, pigment dispersion, and glaucoma in D2 mice. Invest Ophthalmol Vis Sci. 1998; 39:951–962. [PubMed: 9579474]

Kasumu A, Bezprozvanny I. Deranged Calcium Signaling in Purkinje Cells and Pathogenesis in Spinocerebellar Ataxia 2 (SCA2) and Other Ataxias. Cerebellum. 2010 in the press.

Keirstead SA, Miller RF. Calcium waves in dissociated retinal glial (Müller) cells are evoked by release of calcium from intracellular stores. *Glia.*. 1995; 14:14–22. [PubMed: 7615342]

Križaj D, Lai FA, Copenhagen DR. Ryanodine stores and calcium regulation in the inner segments of salamander rods and cones. J Physiol. 2003; 547:761–774. [PubMed: 12562925]

Lam TT, Kwong JM, Tso MO. Early glial responses after acute elevated intraocular pressure in rats. Invest Ophthalmol Vis Sci. 2003; 44:638–645. [PubMed: 12556393]

Li Y, Holtzclaw LA, Russell JT. Müller cell $Ca^{2+}$ waves evoked by purinergic receptor agonists in slices of rat retina. J Neurophysiol. 2001; 85:986–994. [PubMed: 11160528]

Libby RT, Anderson MG, Pang IH, Robinson ZH, Savinova OV, Cosma IM, Snow A, Wilson LA, Smith RS, Clark AF, John SW. Inherited glaucoma in DBA/2J mice: pertinent disease features for studying the neurodegeneration. Vis Neurosci. 2005; 22:637–648. [PubMed: 16332275]

Lucki I, Dalvi A, Mayorga AJ. Sensitivity to the effects of pharmacologically selective antidepressants in different strains of mice. Psychopharmacology (Berl). 2001; 155:315–322. [PubMed: 11432695]

Lundkvist A, Reichenbach A, Betsholtz C, Carmeliet P, Wolburg H, Pekny M. Under stress, the absence of intermediate filaments from Müller cells in the retina has structural and functional consequences. J Cell Sci. 2004; 117:3481–3488. [PubMed: 15226376]

Mandal A, Shahidullah M, Delamere NA. Hydrostatic pressure-induced release of stored calcium in cultured rat optic nerve head astrocytes. Invest Ophthalmol Vis Sci. 2010; 51:3129–3138. [PubMed: 20071675]

Marc RE, Jones BW, Watt CB, Strettoi E. Neural remodeling in retinal degeneration. Prog Retin Eye Res. 2003; 22:607–655. [PubMed: 12892644]

Medina-Ortiz WE, Gregg EV, Brun-Zinkernagel AM, Koulen P. Identification and functional distribution of intracellular Ca channels in mouse lacrimal gland acinar cells. Open Ophthalmol. 2007; 1:8–16.

Misra V, Lee H, Singh A, Huang K, Thimmulappa RK, Mitzner W, Biswal S, Tankersley CG. Global expression profiles from C57BL/6J and DBA/2J mouse lungs to determine aging-related genes. Physiol Genomics. 2007; 31:429–440. [PubMed: 17726092]

Nedergaard M, Rodríguez JJ, Verkhratsky A. Glial calcium and diseases of the nervous system. Cell Calcium. 2010; 47:140–149. [PubMed: 20045186]

Newman EA. Propagation of intercellular calcium waves in retinal astrocytes and Müller cells. J Neurosci. 2001; 21:2215–2223. [PubMed: 11264297]

Niebauer M, Gruenthal M. Neuroprotective effects of early vs. late administration of dantrolene in experimental status epilepticus. Neuropharmacology. 1999; 38:1343–1348. [PubMed: 10471088]

Ouardouz M, Nikolaeva MA, Coderre E, Zamponi GW, McRory JE, Trapp BD, Yin X, Wang W, Woulfe J, Stys PK. Depolarization-induced $Ca^{2+}$ release in ischemic spinal cord white matter involves L-type $Ca^{2+}$ channel activation of ryanodine receptors. Neuron. 2003; 40:53–63. [PubMed: 14527433]

Panagis L, Zhao X, Ge Y, Ren L, Mittag TW, Danias J. Gene expression changes in areas of focal loss of retinal ganglion cells in the retina of DBA/2J mice. Invest Ophthalmol Vis Sci. 2010; 51:2024–2034. [PubMed: 19737878]

Popescu BO, Oprica M, Sajin M, Stanciu CL, Bajenaru O, Predescu A, Vidulescu C, Popescu LM. Dantrolene protects neurons against kainic acid induced apoptosis in vitro and in vivo. J Cell Mol Med. 2002; 6:555–569. [PubMed: 12611640]

Puk O, Dalke C, Hrabé de Angelis M, Graw J. Variation of the response to the optokinetic drum among various strains of mice. Front Biosci. 2008; 13:6269–6275. [PubMed: 18508659]

Punzo C, Cepko C. Cellular responses to photoreceptor death in the rd1 mouse model of retinal degeneration. Invest Ophthalmol Vis Sci. 2007; 48:849–857. [PubMed: 17251487]

Rentería RC, Strehler EE, Copenhagen DR, Krizaj D. Ontogeny of plasma membrane Ca2+ ATPase isoforms in the neural retina of the postnatal rat. Vis Neurosci. 2005; 22:263–74. [PubMed: 16079002]

Ryskamp DA, Witkovsky P, Barabas P, Huang W, Koehler C, Akimov NP, Lee SH, Chauhan S, Xing W, Rentería RC, Liedtke W, Krizaj D. The Polymodal Ion Channel Transient Receptor Potential

Vanilloid 4 Modulates Calcium Flux, Spiking Rate, and Apoptosis of Mouse Retinal Ganglion Cells. J Neurosci. 2011; 31:7089–7101. [PubMed: 21562271]

Shoshan-Barmatz V, Zakar M, Shmuelivich F, Nahon E, Vardi N. Retina expresses a novel variant of the ryanodine receptor. Eur J Neurosci. 2007; 26:3113–3125. [PubMed: 18005065]

Singh SM, Treadwell J, Kleiber ML, Harrison M, Uddin RK. Analysis of behavior using genetical genomics in mice as a model: from alcohol preferences to gene expression differences. Genome. 2007; 50:877–897. [PubMed: 18059552]

Soto I, Oglesby E, Buckingham BP, Son JL, Roberson ED, Steele MR, Inman DM, Vetter ML, Horner PJ, Marsh-Armstrong N. Retinal ganglion cells downregulate gene expression and lose their axons within the optic nerve head in a mouse glaucoma model. J Neurosci. 2008; 28:548–561. [PubMed: 18184797]

Steele MR, Inman DM, Calkins DJ, Horner PJ, Vetter ML. Microarray analysis of retinal gene expression in the DBA/2J model of glaucoma. Invest Ophthalmol Vis Sci. 2006; 47:977–985. [PubMed: 16505032]

Stirling DP, Stys PK. Mechanisms of axonal injury: internodal nanocomplexes and calcium deregulation. Trends Mol Med. 2010; 16:160–170. [PubMed: 20207196]

Whitmore AV, Libby RT, John SW. Glaucoma: thinking in new ways-a rôle for autonomous axonal self-destruction and other compartmentalised processes? Prog Retin Eye Res. 2005; 24:639–662. [PubMed: 15953750]

Xue LP, Lu J, Cao Q, Hu S, Ding P, Ling EA. Muller glial cells express nestin coupled with glial fibrillary acidic protein in experimentally induced glaucoma in the rat retina. Neuroscience. 2006b; 139:723–732. [PubMed: 16458441]

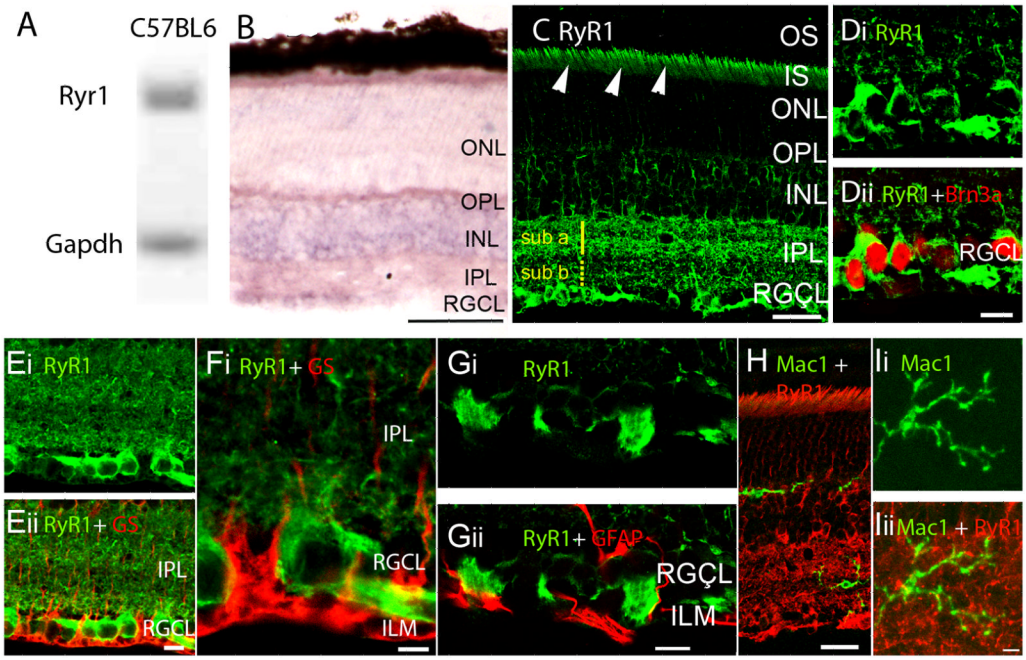


**Figure 1.**

RyR1 gene expression, mRNA and protein distribution in the B6 retina. (A) Amplicons for *RyR1* and glyceraldehyde-3-phosphate dehydrogenase (*Gapdh*) isolated from the total retinal pool and separated on a 20% agarose gel. (B) In situ hybridization analysis of 12 month-old B6 retinas exposed to *RyR1* antisense probes. The reaction product is localized to perikarya in INL and RGC layers. Weak labeling is seen in the ONL, with the labeling of rod inner segments by the antisense probe. Radial processes spanning the retina are weakly labeled. Scale bar =50 μm. (C) RyR1 localization in an adult (9 month-old) B6 retina. The RyR1 antibody labels rod ellipsoids and inner segments (arrowheads), perikarya within the INL, RGCL and the IPL; RyR1-ir in the sublamina a is more pronounced compared to sublamina b. Scale bar =20 μm. (D) 12 months-old retina. RyR1 signal in the RGCL colocalizes with the RGC marker Brn3a. (E – G) 15 months-old retina. RyR1 signal in the RGCL and ILM shows little colocalization with glutamine synthetase (GS) or GFAP. Scale bar =10 μm. (H & I) RyR1-ir does not colocalize with the microglial marker Mac-1. Scale bar =20 μm in H, 10 μm in I.

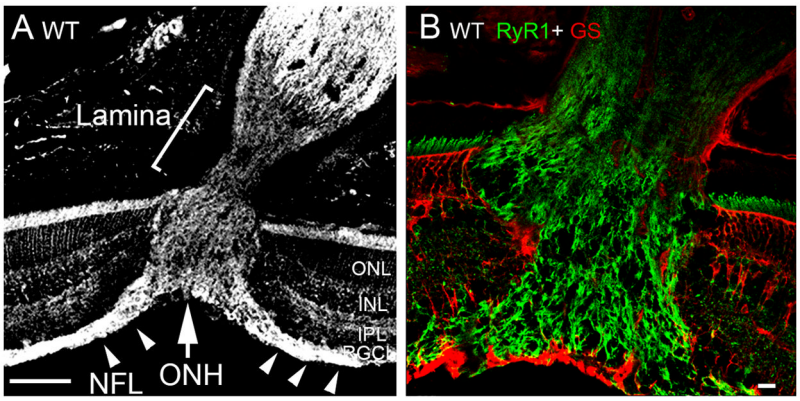


**Figure 2.**
B6 retinas, RyR1 expression in the optic nerve head. (A) The RyR1 antibody labels the retinal nerve fiber layer (NFL; arrowheads), the ONH (arrow) and the myelinated portion of the optic nerve whereas RyR1 expression in the astrocyte lamina is modest. Scale bar =100 μm. (B) Double labeling for RyR1 and GS shows little GS signal within the ONH of the B6 retina. Scale bar =10 μm.

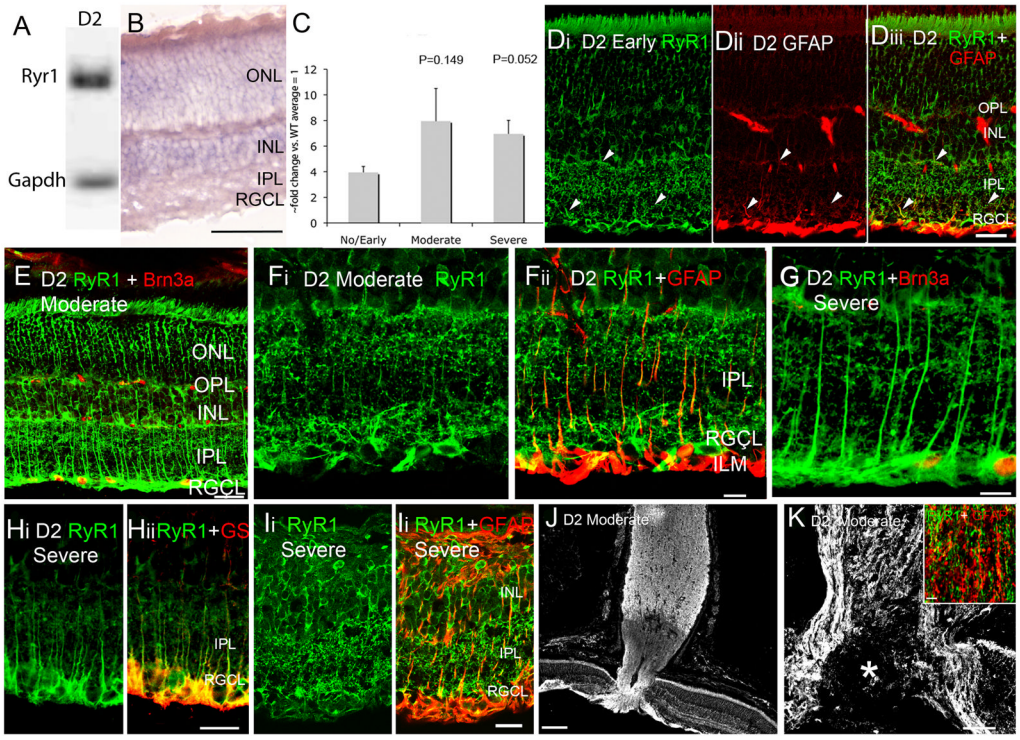


**Figure 3.**

RyR1 expression in D2 retina. (A) PCR products for *RyR1* and *Gapdh* mRNA from the total retinal pool. (B) D2 retinas labeled by the *RyR1* antisense probe. The reaction product is localized to perikarya in INL and RGC layers. The antisense probe weakly labels the ONL, rod inner segments and radial processes spanning the retina. Scale bar =50 μm. (C) RT-PCR for *RyR1*, expressed as ~fold change with respect to age-matched B6 retinas. (D) RyR1 and GFAP localization in No/Early glaucoma D2 retina. Some, but not all, radial RyR1-ir processes expressed GFAP (arrowheads). (E) Moderate glaucoma retina, double labeled for RyR1 and BRN3a, a Z-stack from 12 consecutive sections. Scale bar =20 μm. (F) Moderate glaucoma. There is an upregulation and partial colocalization of RyR1- and GFAP-ir processes in the IPL and the ILM/RGCL. Scale bar = 20 μm. (G) Severe glaucoma, double labeled for RyR1 and Brn3a. Scale bar =10 μm. (H) Severe glaucoma, retina labeled for RyR1 and glutamine synthetase. Scale bar =20 μm. (J) Severe glaucoma in a 15 month old D2 retina exhibiting glial hypertrophy and retinal remodeling. Scale bar =10 μm. (J & K) ONH regions from two moderate glaucoma eyes. (J) The RyR1 antibody labels the NFL, ONH and the myelinated region of the optic nerve. Scale bar =100 μm. (K) Moderate glaucoma. RyR1 signal surrounds the excavated region within the ONH (asterisk). *Inset*: Severe glaucoma. Double labeling of the glial laminar region in the optic nerve shows modest colocalization between RyR1 and GFAP signals. Scale bar =10 μm.

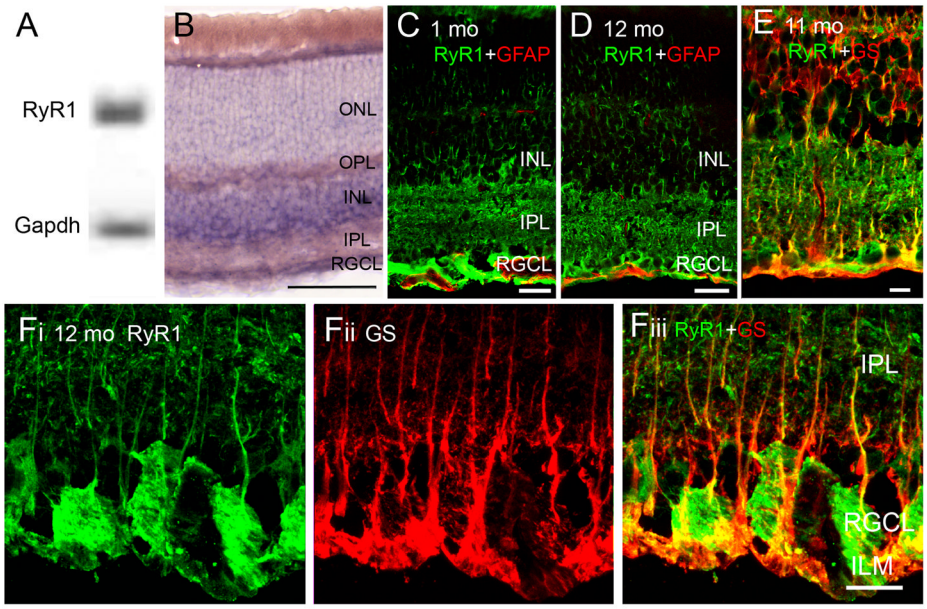


**Figure 4.**

RyR1 expression in D2-*Gpnmb*$^{+}$ retinas. (A) PCR products for *RyR1* and *Gapdh* mRNA from the total retinal pool. (B) In situ hybridization signals in D2-*Gpnmb*$^{+}$ retinas show similar localization to B6 and D2 retinas. Scale bar = 50 μm. (C & D) 1 month and 12 months-old retinas, double labeled for RyR1 and GFAP show little colocalization. Scale bars = 20 μm (E–F) A subset of 11–12 months-old D2-*Gpnmb*$^{+}$ retinas showed RyR1-ir signals within the ILM and IPL regions. These processes colocalized with glutamine synthetase. Scale bars = 10 μm.

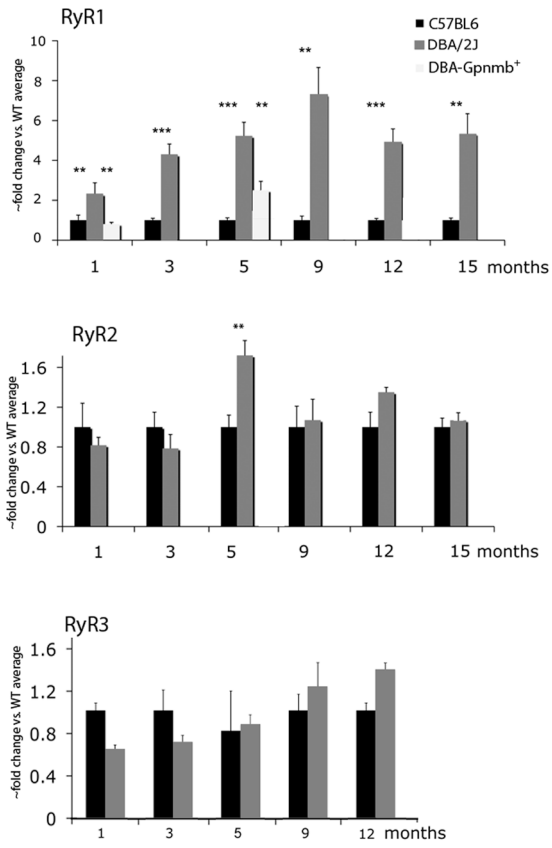


**Figure 5.**

RyR gene expression in B6 and D2 retinas. (A) RT-PCR. RyR1 transcripts are strongly upregulated in D2 compared to B6 retinas. Analysis of D2-*Gpnmb*$^{+}$ samples shows no difference from B6 expression at 1 month but a significant upregulation at 5 months. (B) RyR1 transcript levels in D2 retinas with moderate and severe glaucoma are elevated in comparison to No/Early glaucoma. (C & D) RyR2 and RyR3 mRNA levels show no consistent differences between B6 and D2 retinas.

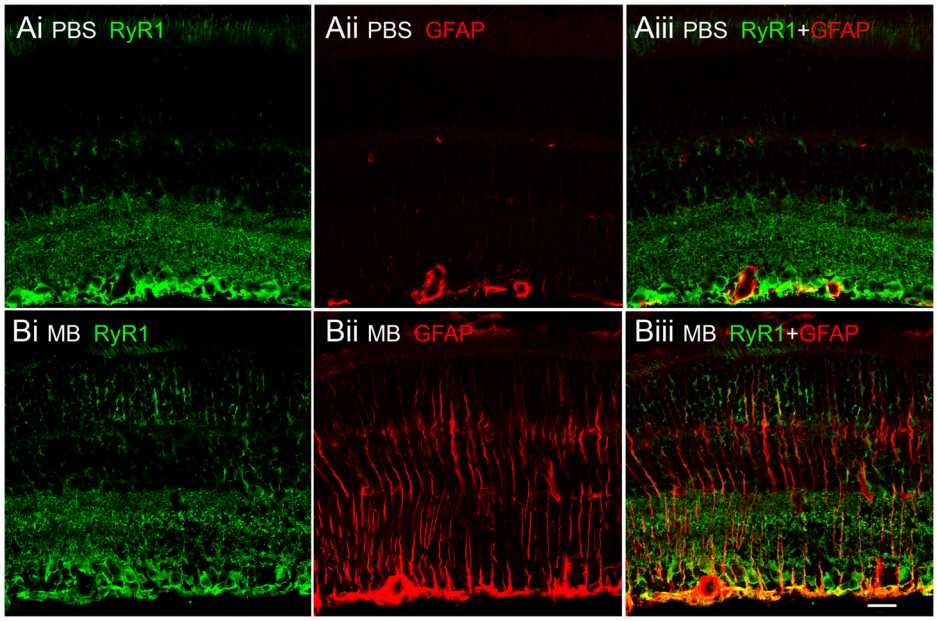


**Figure 6.**

Acute glaucoma model. B6 eyes were injected with PBS (A) or microbeads (B) and colabeled with RyR1 and GFAP antibodies. Microbead-injected eyes exhibited prominent GFAP-ir which showed partial colocalization with RyR1. In contrast, no colocalization was observed in sham controls.

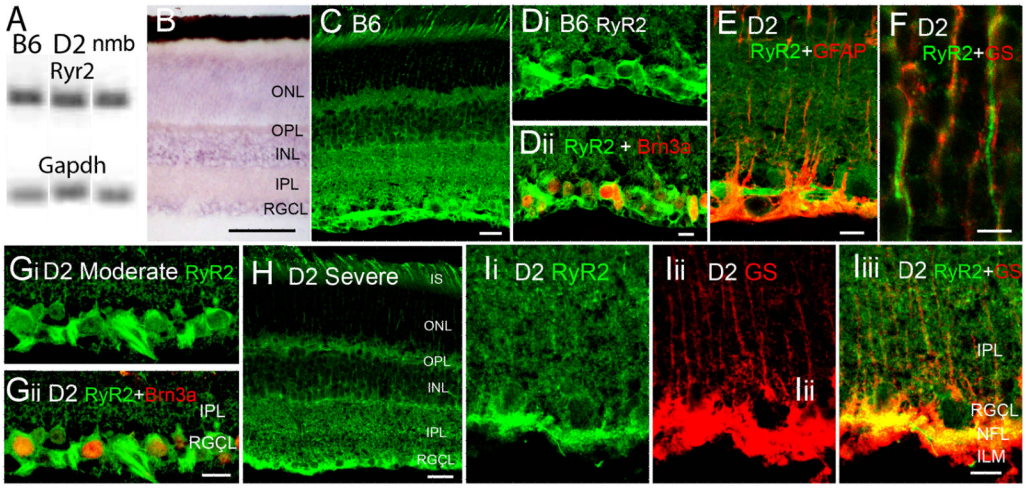


**Figure 7.**

RyR1 expression and localization in B6m D2 and D2-*Gpnmb*$^{+}$ retinas. (A) PCR amplicons for *RyR2* and *Gapdh*. (B) ISH for *RyR2*. The reaction product is localized to perikarya in INL, RGCL and distal ONL. Scale bar =50 μm. (C & D) RyR2 immunolocalization in the adult B6 retina. The RyR2 antibody labels all retinal layers, with a prominent signal in the RGCL. (E–I) D2 retinas. (E) Inner retina. Double labeling for RyR2 and GFAP shows little colocalization. Scale bar =10 μm. (F) Outer retina. Double labeling for RyR2 and glutamine synthetase in the ONL. RyR2-ir photoreceptor processes do not colocalize with radial processes of GS-ir Müller cells. Scale bar =5 μm. (Gi & ii) Moderate glaucoma, double labeling for RyR2 and Brn3a. The RyR2 antibody labels cell bodies of RGCs (arrowheads) and axonal processes in the NFL (arrow). Scale bar =10 μm. (H) Severe glaucoma. Scale bar =20 μm. (Ii-iii) Severe glaucoma. Double labeling for RyR2 and GS shows little colocalization in the IPL. Scale bar =10 μm.

**Table I**

List of forward and reverse primers used for RT-PCR analysis. The RyR1 gene was tested with two separate sets of primers.

| Gene | Forward | Reverse |
|---|---|---|
| **Gapdh** | ACT TCA ACA GCA ACT CCC ACT CTT C | GGG TGG TCC AGG GTT TCT TAC TC |
| **RyR1-A** | AGT CAA GAC GCT CCG CAC CAT C | GGC TCG TCC TCA TCT TCG CTC TT |
| **RyR1-B** | TAC TTC GAC ACA ACC CCA CA | ACA GTC TCC AGC AGG GAA GA |
| **RyR2** | CTA CCC GAA CCT CCA GCG ATA CT | GCA AAA GAA GGA GAT GAT GGT GTG |
| **RyR3** | ATG AGC CGG ATA TGA AGT GTG ACG A | TGA ATG ATG GCC AGC AAG ATG AC |
| **Brn3a** | AGA GAC AGA AGC AGA AGC GGA TGA | GCC CCC AAA TGA GAG CAG AAA CTT |
| **Gfap** | GGA CAT CGA GAT CGC CAC CTA CAG | TGA CCT CAC CAT CCCGCA TCT C |